ORIGINAL PAPER

Calotropis procera: UHPLC-QTOF-MS/MS based profiling of bioactives, antioxidant and anti-diabetic potential of leaf extracts and an insight into molecular docking

Muhammad Nadeem[1] · Muhammad Waseem Mumtaz[1] · Muhammad Danish[1] · Umer Rashid[2] · Hamid Mukhtar[3] · Farooq Anwar[4] · Syed Ali Raza[5]

Abstract

This work aims to investigate antioxidant/antidiabetic activities of aqueous and aqueous ethanol (20–80% ethanol:water, v/v) extracts from *Calotropis procera* leaves followed by profiling of related bioactives using UHPLC-QTOF-MS/MS technique. Of the extracts produced, 80% ethanolic extract offered highest level of total phenolics and total flavonoids with contribution 176.31 ± 2.09 mg GAE/g DE and 65.38 ± 2.65 mg RE/g DE, respectively. The α-Glucosidase and α-amylase inhibitory effect of 80% extract was found to be maximum with IC_{50} value of 0.78 ± 0.01 mg/mL and 0.93 ± 0.01 mg/mL, respectively among others. The same extract also showed higher total antioxidant power (184.91 ± 3.65 mg/g AAE) and antiradical effect with corresponding IC_{50} of 87.35 ± 2.45 μg/mL. UHPLC-QTOF-MS/MS investigation of 80% ethanolic extract led to identification/characterization of different antioxidant and antidiabetic metabolites such as *p*-hydroxybenzoic acid, 4-O-*β*-D-galactopyranosyl-D-fructose, myrciacitrin IV, quinic acid and astragaloside/kaempferol/quinic acid derivatives. Based on the present findings, 80% ethanol leaf extract of *C. procera* was found to be an important source of bioactives with significant potency of antioxidant, α-glucosidase and α-amylase enzyme inhibitory effects. Binding affinity data and interaction patterns, elucidated via docking simulations, of potential bioactives in *C. procera* leaf extract predicted that they can inhibit α-glucosidase and α-amylase synergistically to prevent hyperglycemia. These results explore potential uses of *C. procera* for development of functional foods and antioxidant/antidiabetic nutraceuticals.

Keywords Antidiabetic · Antioxidant · *Calotropis procera* · Functional food · Phenolics · UHPLC-QTOF-MS/MS

Introduction

Plants are recognized as one of the richest sources of bioactive constituents and high-value macro/micronutrients with nutraceutical/pharmaceutical potential [1]. Recently, with developments in area of optimal nutrition, there is revival of interest for using plants as a potent source of food and medicines [2, 3]. There is an emerging trend in using herbal dietary supplements or entire plants for combating cancer, diabetes, obesity and cardiovascular disorders [4]. In particular, a direct association has been documented between the ingestion of specific plant food such as fruits, vegetables or grains and reduced prevalence of diabetes and other degenerative diseases [5-7].

Diabetes mellitus (especially type-2) is considered a severe metabolic health problem, characterized by hyperglycemia. Clinical trials have shown that diabetes mellitus exerts serious negative effects on human's health such as hypertension, kidney failure, premature death, frailty and depression etc. [7, 8]. According to estimates this disease can affect up to 592 million people in the world till 2035 [9]. International Diabetes Federation (IDF) has reported that Pakistan may become 7th world's largest country with

✉ Muhammad Waseem Mumtaz
muhammad.waseem@uog.edu.pk

[1] Department of Chemistry, University of Gujrat, Gujrat, Pakistan

[2] Department of Chemistry, COMSATS University Islamabad, Abbottabad Campus, Abbottabad, Pakistan

[3] Institute of Industrial Biotechnology, GC University, Lahore, Pakistan

[4] Department of Chemistry, University of Sargodha, Sargodha, Pakistan

[5] Department of Chemistry, GC University, Lahore, Pakistan

diabetic inhabitants till 2030. This situation is challenging for both health care policy makers and professionals in Pakistan [10]. An effective approach in managing this chronic disease is to control blood glucose by inhibiting carbohydrate hydrolyzing enzymes (α-amylase/α-glucosidase) in digestive system [11]. Natural enzyme inhibitors are considered to be healthier for the consumers [12] and endorsed by IDF as the first line remedy because of their efficacy and safety [12], compared to synthetic enzyme inhibitors (acarbose/miglitol) which have restricted use due to their adverse health effects [13].

Normal human physiological system also involves the production of reactive oxygen species (ROS), but an imbalance between prooxidants and antioxidants can induce several metabolic disorders such as atherosclerosis, aging, diabetes and cancer [14]. More importantly, the free radicals are also involved in destruction of *β*-cells of pancreas that lead to reduce the insulin level. The disruption in pancreatic function results in elevated blood glucose level. Though synthetic antioxidants, for example BHT and BHA, are available commercially to capture free radicals, but they have undesirable health effects, emphasizing the search of safe natural antioxidants [15].

Calotropis procera (Apocynaceae) is a moderate, dark green wild shrub with wide fleshy leaves. It grows throughout the tropical and warm temperate climates [16]. Traditionally, it is being employed for curing various disorders since ancient times [17]. For example, the latex is employed for curing leprosy, eczema [18], inflammation [19] and bronchial asthma [20]. The flowers are used as a tonic and appetizer [16]. They also have hepatoprotective activity [21]. Fresh roots are used as toothbrush to cure toothache [16] and reported to possess anti-fertility [22] as well as anti-ulcer activity [23]. Leaves of this plant are considered valuable as an antidote for snake bite, rheumatic disorder, viral infection, injuries caused by burn, diarrhea, body pain [24], to cure jaundice [25] and catarrh [16]. Leaves are also reported to have antimalarial [26], anthelmintic [27] and antioxidant activity [28].

Calotropis procera leaves are traditionally being consumed to treat diabetes without proper understanding and knowledge about the scientific basis of its antioxidant, α-amylase and α-glucosidase inhibitory effects. It deems necessary to evaluate the inhibition of dietary enzymes like α-amylase and α-glucosidase for in vitro assessment of antidiabetic potential of *C. procera* leaves and elucidate possible interactions among identified bioactive compounds and active sites of enzymes, offering logical basis for possible enzyme inhibition mechanism by complex mixture of compounds [29]. Currently, key focus of the functional foods/phyto-pharmaceutical industries is to reduce the cost involved in the development of new products and to improve the selectivity, sensitivity and resolution for their

detection. Recently, UHPLC-QTOF-MS/MS has emerged as emphatic and effective analytical tool for rapid screening and characterization of plant metabolites due to its high sensitivity, selectivity, specificity and shorter analysis time etc., comparative to conventional methods which suffer from various drawbacks such as low sensitivity, low resolution, high solvent consumption, long analysis time and need of derivatization [30, 31].

Therefore, the current work was planned to investigate antioxidant, α-glucosidase and α-amylase inhibitory efficacy alongwith profiling of potent bioactives responsible for antidiabetic potential in hydroethanolic leaf extracts of *C. procera* so as to provide scientific evidence for its traditional medicinal uses. In our strategy, we applied UHPLC-QTOF-MS/MS technique to investigate the chemical constituents in the leaf extract of *C. procera*.

After profiling of related bioactives using UHPLC-QTOF-MS/MS technique, we elucidated the synergistic effect of identified metabolites by using molecular docking tool. As per best of our knowledge, this may probably be the first study revealing the binding affinities through molecular docking of phytochemicals from *C. procera* against α-amylase and α-glucosidase. The binding affinity data may be helpful to strengthen the notion about synergistic effect of phyto-constituents of *C. procera* to inhibit α-glucosidase as well as α-amylase activity and impart hyperglycemic attributes. Conclusively, structural information of leaf extracts from *C. procera* enabled us to analyze the role of each constituent and synergistic impact was considered as the functional entity behind the α-glucosidase and α-amylase inhibition.

Materials and methods

Reagents and chemicals

Folin–Ciocalteu (F–C) reagent, gallic acid (GA), DPPH radical, butylated hydroxyanisole (BHA), aluminium chloride (AlCl₃), rutin, sodium nitrite (NaNO₂), sodium hydroxide (NaOH), sulphuric acid (H₂SO₄), *p*-nitrophenyl glucopyranoside (pNPG), sodium phosphate (Na₃PO₄), ammonium molybdate ((NH₄)₂MoO₄), anhydrous sodium carbonate (Na₂CO₃), methyl alcohol (MeOH), ethyl alcohol (EtOH), acarbose, α-amylase, α-glucosidase and ascorbic acid (AA) used were analytical research grade as of Sigma-Aldrich (USA), BDH & Merck (Germany).

Plant material and extraction

Mature *C. procera* leaves were procured from Azad Jammu & Kashmir, Pakistan in June 2017. The voucher specimen (UOG-CHEM-18/2018) was deposited at Department of

Botany, University of Gujrat, Gujrat, Pakistan, further identified and authenticated the species as *Calotropis procera*. Fresh leaves were first washed with water, and after drying with cotton paper, quenched instantly using liquid N_2 to preserve secondary metabolites, followed by freeze drying (Christ-Alpha 1–4, LD freeze dryer, Germany) at -68 °C for 2 days. The dried leaves were then powdered, passed through a 60-mesh sieve and kept in sealed plastic bag at -80 °C till further experiments.

Powdered leaves (10 g) were soaked in 100 mL of ethanol:water solvent systems of various concentrations (Aqueous, 20:80, 40:60, 60:40, 80:20 and 100:0 v/v) at constant conditions of temperature (35 ± 0.2 °C) and humidity ($25 \pm 5\%$) for 48 h. The resulting mixtures were then vortexed for 2 h using mixture (Wise Mix SHO-1D, DAIHAN Scientific, Korea) and sonicated using ultrasonic disintegrator (soniprep 150 ultrasonicator MSE, UK) for almost 1 h at 35 ± 0.2 °C, centrifuged for 10 min (13,000 rpm) and filtered under same experimental conditions. For filtration, the mixtures were transferred to automated assembly of porcelain having Whatman filter paper 42 and equipped with vacuum pump (Todays Rocker 300 vacuum pump). Excessive solvent was evaporated under vacuum using a rotary evaporator (35 °C). The obtained crude extracts were freeze-dried (Christ-Alpha 1–4, LD freeze dryer, Germany) at -68 °C again till constant weight and stored at -80 °C for future use [32]. Percentage yields were calculated and extracts were again stored in a freezer at -80 °C till further use.

Phytochemicals evaluation

Total phenolic contents (TPC)

Determination of TPC in understudy extracts was carried out corresponding to protocol described by Kim et al. [33] with little modification. For this, 0.10 mL of each fraction/extract (1 mg/mL) was added in 1 mL of F–C reagent. After 5 min 3 mL of 10% Na_2CO_3 solution was mixed and the reaction mixture incubated for 90 min at 23 °C; the absorbance was noted at 750 nm (Schimadzu UV-1700 Spectrophotometer, Japan). The amount of TPC was articulated as milligram of gallic acid equivalent/gram dried extracts (mg GAE/g DE).

Total flavonoid contents (TFC)

The spectrophotometric procedure was used for the estimation TFC in the extracts [34, 35]. The sample mixtures were prepared by adding 0.2 mL of plant extracts to the mixtures comprising 0.5 M $NaNO_2$ (0.10 mL), 0.3 M $AlCl_3 \cdot 6H_2O$ (0.15 mL) and 30% MeOH (3.4 mL). After keeping the mixture for at least 5 min, 1 M NaOH (1 mL) was added in it. The absorbance was recorded at 510 nm. TFC were

estimated using rutin (standard) and represented as milligrams of rutin equivalent per gram dried extracts (mg RE/g DE).

DPPH radical scavenging assay

Scavenging potential of samples/extracts was investigated in accordance to an already reported method by Mensor et al. [36]. The antioxidant activity was articulated as IC_{50} (µg/mL). All experiments were conducted thrice and results were indicated as mean $\pm$ standard deviation (SD). BHA was used as reference standard/ positive control. The extracts at various concentrations were mixed with 500 µL DPPH solution in CH_3OH. After keeping reaction mixtures for 15 min at 30 °C, absorbance was taken at 517 nm. Percent radical scavenging effect was evaluated by following equation:

$$\text{Scavenging effect (\%)} = \left(\frac{\text{Control}_{\text{absorbance}} - \text{Sample}_{\text{absorbance}}}{\text{Control}_{\text{absorbance}}} \right) \times 100$$

Total antioxidant power (TAP) assay

TAP of the crude plant extracts was detected by phosphomolybdenum assay as described by Umamaheswari and Chatterjee [37]. Briefly, 0.10 mL of each extract was carefully dissolved in reagent solution (28 mM of Na_3PO_4 + 4 mM of $(NH4)_2MoO_4$ + 0.6 M of H_2SO_4) in vials. After incubation at 90 °C for 90 min in water bath, reaction mixtures were cooled to 30 °C and absorbance was recorded at 765 nm.

The α-amylase inhibitory assay

Inhibitory effects of different hydro-alcoholic extracts of *C. procera* leaves against α-amylase were evaluated concurring to method described by Shai et al. [38] with slight modification. Varying amounts of extracts were mixed with an optimum volume (2 units/mL) of enzyme in 0.10 M Na_3PO_4 buffer having pH of 6.8. After heating at 37 °C for about 20 min in water bath, starch solution (1%) was added into the mixture and again heated at 37 °C for 1 h. Then 0.1 M NaOH (2000 µL) was added into the mixture for reaction termination. The absorbance of final reaction mixture was read using spectrophotometer at 540 nm. The α-amylase inhibitory potential was measured as percentage of the positive control without inhibitor.

$$\alpha\text{-amylase inhibition (\%)} = \left(\frac{A_{540} \text{ control} - A_{540} \text{ sample}}{A_{540} \text{ control}} \right) \times 100$$

IC_{50} values (concentrations showing 50% inhibition in mg/mL) of extracts were calculated graphically. Acarbose was taken as reference inhibitor/positive control.

The α-glucosidase inhibitory assay

In vitro anti-alpha-glucosidase potential of the tested extracts was evaluated according to a method stated by Jabeen et al. [39] with modification. Briefly, sample mixtures containing 70 µL of 30 mM phosphate buffer (pH of 6.8), 10 µL of crude extract, 10 µL α-glucosidase enzyme were place in reaction flask. Every reaction mixture was incubated at room temperature for 15 min, and reaction initiation was carried out by adding 10 µL of 5 mM pNPG in each mixture. After re-incubation for 30 min, 2 mL of Na_2CO_3 (0.1 M) was added to terminate the reaction and absorbance was taken at 405 nm, spectrophotometrically. Measurements were performed thrice and percentage inhibitions was calculated using following formula:

α-glucosidase inhibition (%)

$$= \left(\frac{A_{405} \text{ control} - A_{405} \text{ sample}}{A_{405} \text{ control}} \right) \times 100$$

Acarbose was taken as reference inhibitor/positive control and findings were represented as IC_{50} (mg/mL).

UHPLC-Q-TOF–MS/MS analysis

Based upon data of different assays, the most potent extract (80% ethanolic extract) was dissolved in $MeOH_{(aq)}$ and filtered using Poly (tetrafluoroethylene) filter of pore size 0.45 µm. The prepared extract sample was analyzed by UHPLC-QTOF-MS/MS for identification of bioactive constituents. A scanning range starting from 50 to 1200 m/*z* was set for MS/MS analysis by means of negative ionization mode. Thermo Hypersil UHPLC GOLD column (3 µm × 2.1 mm × 100 mm) was used. Gradient mobile phase containing acetonitrile (CH_3CN) and H_2O (with 0.1% HCOOH and 5 mM $HCOONH_4$) was applied. Gradient programming/elution was started from 10 to 90% CH_3CN for a time 0.01–8.0 min, with mobile phase flow rate of 0.8 mL/min and injection volume of 20 µL. Explanation of data was assured using Sciex Peak views 2.1 soft-ware, ACD/Lab and Chemispider/PubChem data-base. Peaks resolved were recognized further by their base peaks, precise masses, fragmentation pathways and comparison with literature data.

Docking studies

Docking studies were performed, using Molecular Operating Environment (MOE 2016.08). For α-glucosidase enzyme, docking study was done on homology-modelled α-glucosidase reported by our research group [40]. Three-dimensional structure of porcine pancreatic α-amylase (PPA) complexed with acarbose was downloaded from Protein Data Bank (PDB code 1OSE). Preparation of ligands

downloaded enzymes (Three-dimensional protonation, energy minimization and determination of binding site) was carried out by our previously reported methods [40, 41]. The interpretation of docking results as well as analysis of their surfaces with graphical representation was completed using MOE and discovery studio visualizer [42].

Statistical analysis

The experimental values were recorded in triplicate and standard deviation ($\pm$) was calculated. The ANOVA was applied to evaluate the level of significance difference of means by using Minitab 17.0 statistical software.

Results and discussion

### Extract yields (%), TPC and TFC

The effect of solvent composition on extraction yield is shown as Fig. 1.

Highest extract yield of $20.98 \pm 0.45\%$ was attained when extraction process was performed with 80% ethanol (80:20 ethanol:water, v/v). The least extract yield ($14.38 \pm 0.24\%$) was given by pure aqueous solvent system. The extract yield gradually increased by increasing ethanol component of solvent mixture and maximum yield was obtained at 80% ethanol. However, a sharp decrease in extract yield was observed with 100% ethanol. The statistical analysis indicated that extract yield given by 80% ethanol was significantly higher among others ($p < 0.05$). The differences in extract yields were probably due to the variable solvent polarity induced by solvent components. The water is believed as potential swelling agent for plant material while ethanol is thought to be involved in bond breakage of metabolite in plant matrix. The water and ethanol in combination produced significantly higher extract yields in previous studies involving extraction of phytochemicals from plant materials [43].

Phenols are imperative plant bioactives because of their scavenging capability and physiological functions. The structural interactions of phenolics contribute directly to antioxidant activity of plants [44]. Similarly, flavonoids also play a dynamic role in preserving *β*-cells integrity/function by scavenging free radicals [45] and prevent/reduce the oxidative damage encountered in human degenerative diseases such as cancer, diabetes and hypertension [12, 46]. So, it is important to investigate the polyphenol and flavonoid contents for estimation of antioxidant/antidiabetic potential. The findings of current research regarding total phenolic and flavonoids in leaves of *C. procera* are shown in Table 1.

Maximum level of TPC and TFC was recorded in 80% ethanol extract (176.31 ± 2.09 mg GAE/g DE, 65.38 ± 2.65 mg RE/g DE) followed by 60% extract

Fig. 1 Extract yields from leaves of *C. procera*. Values sharing different letters varied considerably ($p < 0.05$)
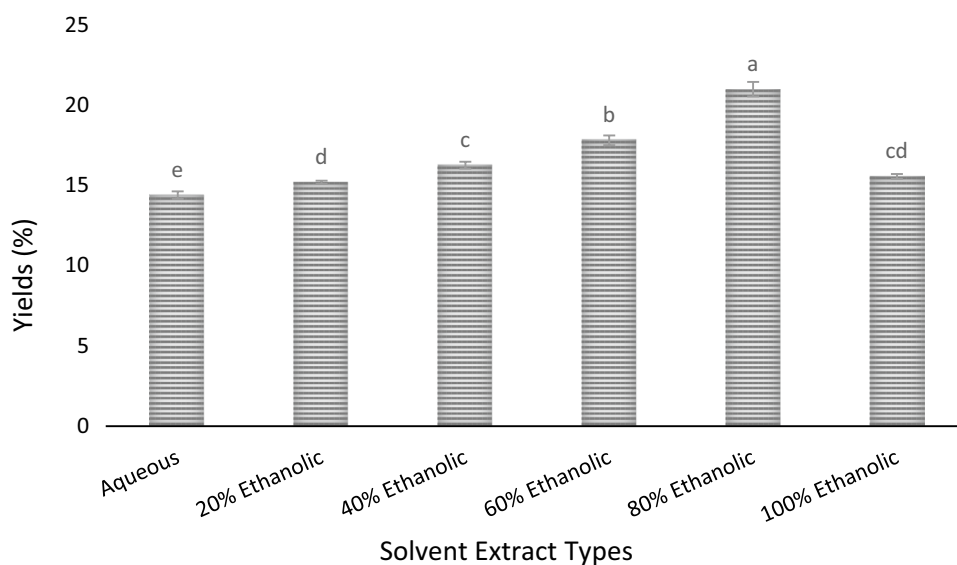
Table 1 TPC and TFC in leaf extracts of *C. procera*

Extracts	TPC in mg GAE/g DE	TFC in mg RE/g DE
Aqueous	53.67 ± 1.68^f	25.48 ± 1.10^e
20% ethanol	75.53 ± 2.12^e	37.60 ± 2.42^d
40% ethanol	128.61 ± 2.37^c	44.59 ± 1.70^c
60% ethanol	135.22 ± 1.61^b	55.15 ± 0.90^b
80% ethanol	176.31 ± 2.09^a	65.38 ± 2.65^a
100% ethanol	86.56 ± 2.05^d	45.05 ± 2.55^c

Different alphabets given as superscript (a–f) with in the same columns represent significant variation of mean among extraction solvents ($p < 0.05$)

(135.22 ± 1.61 mg GAE/g DE, 55.15 ± 0.90 mg RE/g DE). The lowest value of TPC and TFC was detected where pure water was used as extraction solvent (53.67 ± 1.68 mg GAE/g DE, 25.48 ± 1.10 mg RE/g DE). A higher yield of phenolics from 80% ethanol extract can be linked to compatibility and polarity of this solvent system. The statistical investigation exposed significant variations ($p < 0.05$) of TPC and TFC among different extraction media. The strong correlation between phenolics and antioxidant activity of plant extracts is well accepted according to several studies [47]. The stability of plant extracts is one of the challenging issues to be addressed in the development of functional food and pharmaceutical products. Functional foods with added bioactive plant extract(s) should have acceptable food structure, organoleptic flavor, composition,

and stability that is supportive for their traceability and authenticity. Extraction carried out by conventional methods including maceration, soxhlet extraction, solid–liquid, and liquid–liquid extraction etc., might be associated with detrimental repercussions on BACs (biologically active compounds) in plant extracts due to thermal instability, so can be either degraded or completely lost during the preparation of extracts [48]. On the other side, modern extraction methods (green extraction methods) including; ultrasonicated-assisted extraction, microwave- assisted extraction, supercritical-fluid extraction and pressurized-liquid extraction have gained much attention in recent years due to their high extraction yields, selectivity and stability of the target extracts [49]. Furthermore, freeze drying (lyophilization) is a low temperature ($-80\ °C$ to $-20\ °C$) dehydration process used to manufacture about 50% of biopharmaceuticals. In freeze-drying, chemical or physical degradation reactions are inhibited or sufficiently decelerated, resulting in an improved long-term stability of the extracts [50]. In current research work, we first lyophilized the plant leaves after quenching with liquid nitrogen followed by UAE (ultrasonic- assisted extraction) and lyophilization of recovered extracts to ensure the stability of extracted bioactives.

In vitro antioxidant activity

Low level of antioxidants in the living systems support age related ailments including atherosclerosis, Alzheimer's
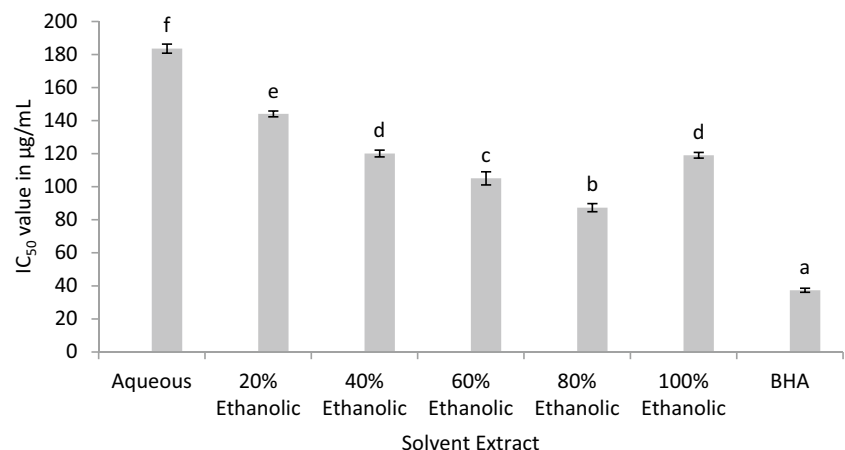
disease, diabetes and cancers. A plausible solution for this dilemma is enrichment of foods with antioxidants that are present in plants [51] and exhibit vital role in scavenging ROS generated due to oxidative stress [52]. In the present research for comprehensive assessment of antioxidant potency of leaves of *C. procera* different antioxidant assays were employed.
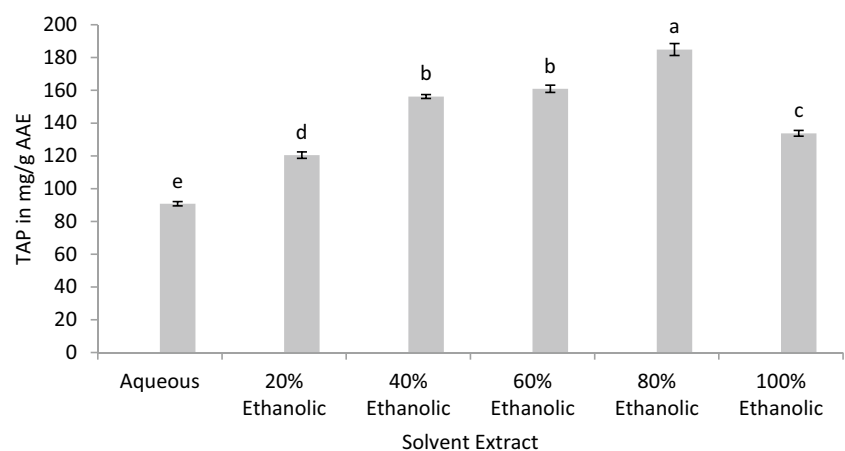
DPPH scavenging assay

DPPH scavenging assay is a commonly adopted method to estimate antioxidant potential of plant extracts/fractions. The results of DPPH assay are given as Fig. 2.

All the tested solvent extracts exhibited ability to quench/reduce DPPH free radicals. The lowest IC_{50} value of 87.35 ± 2.45 μg/mL for antiradical effect was exhibited by 80% ethanolic extract compared to 60% (105.95 ± 3.97 μg/mL), 100% (119.07 ± 1.71 μg/mL), 40% (120.10 ± 2.02 μg/mL) and 20% (144.09 ± 1.73 μg/mL) fractions. The pure aqueous extract showed least DPPH scavenging ability with high IC_{50} value which was 183.58 ± 2.73 μg/mL.

As expected, 80% ethanol extract, rich in phenolic compounds, had the highest capacity towards scavenging DPPH free radicals by donating electron or proton. The statistical analysis indicated that 80% ethanol extract has significantly higher free radical scavenging compared with others counter parts. However, none of the extracts showed antiradical activity comparable with positive control BHA ($IC_{50} = 37.33 \pm 1.20$ μg/mL) ($p < 0.05$).

Total antioxidant power (TAP) assay

The chemistry behind TAP assay involves reduction of Mo (VI) into Mo (V) by any antioxidant. TAP predicts the magnitude of total antioxidants, both water and fat soluble. This assay is used frequently to estimate antioxidant potential of plant extracts/bioactive fractions [53]. TAP of extracts of various concentration are represented as Fig. 3.

As can be seen from the given results, 80% ethanolic extract of *C. procera* leaves (184.91 ± 3.65 mg/g AAE) had considerably higher total antioxidant ability than 60% (160.96 ± 2.19 mg/g AAE), 40% (156.23 ± 1.15 mg/g AAE),

Fig. 2 DPPH scavenging by *C. procera* leaf extracts. Data are statistically significant at $p < 0.05$

Fig. 3 TAP assay results of *C. procera* leaf extracts. Superscripts (a to e) indicate significance difference

100% (133.76 ± 1.75 mg/g AAE), 20% (120.45 ± 1.94 mg/g AAE) and pure aqueous (90.8 ± 1.32 mg/g AAE) extract. The statistical analysis revealed that the difference of means among 80% ethanolic extract and other extracts was significant ($p < 0.05$). However, the difference of means in 60% and 40% ethanolic extract was very low and statistically non-significant ($p > 0.05$). The maximum antioxidant potency of 80% extract compared to other extracts could be due to presence of higher levels of antioxidants.
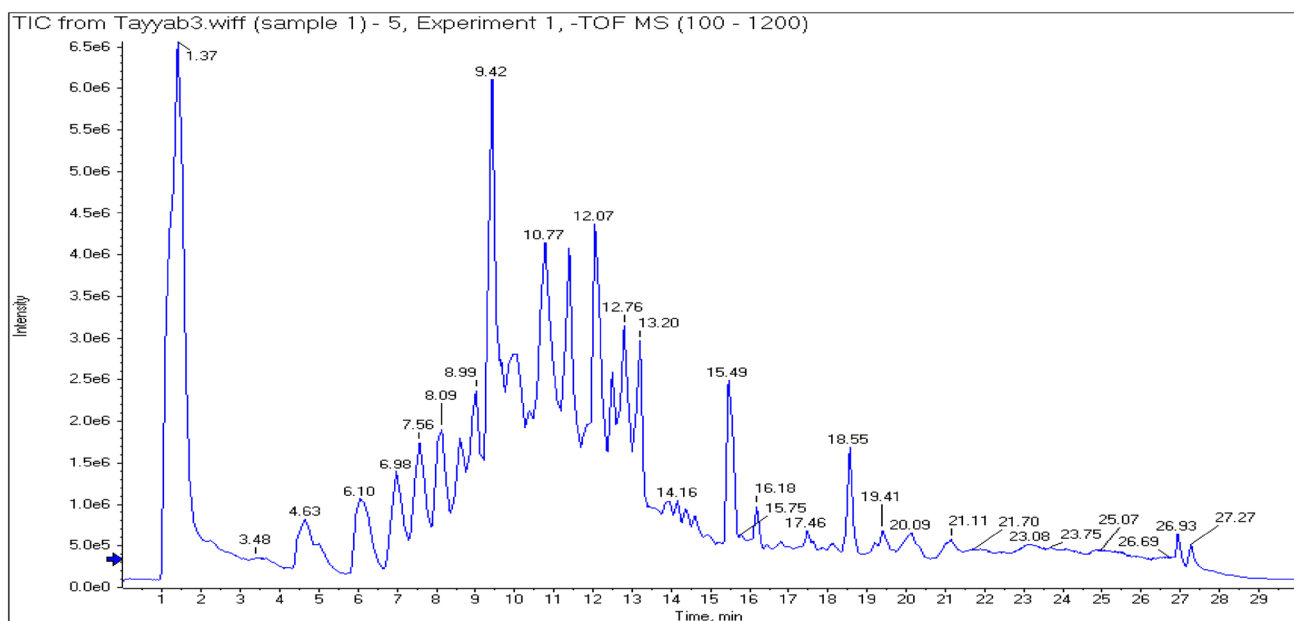
In vitro antidiabetic potential

Both α-amylase and α-glucosidase are dietary enzymes which digest complex carbohydrates and convert them into simpler sugars to accelerate their absorption in intestine.

The inhibition of these enzymes delays the simplification of carbohydrates into glucose which consequently reduces the postprandial blood glucose [54]. α-Glucosidase and α-amylase inhibitors are an effective tool to prevent blood glucose level to rise. Many synthetic inhibitors of these enzymes are available but acarbose is the most studied and extensively used inhibitor of α-amylase/α-glucosidase. However, acarbose like other synthetic drugs is associated with some serious side complications and adopts competitive mode of action [55]. These factors collectively build emphasis to search novel enzyme inhibitors for diabetes management. Plants, being rich source of natural α-amylase and α-glucosidase, may solve this purpose. The inhibitory values of *C. procera* extracts against these enzymes are represented in Table 2.

The results indicated that among the tested extracts, 80% ethanolic extract inhibited the activity of α-glucosidase and α-amylase to maximum extent with lowest IC_{50} values of 0.78 ± 0.01 and 0.93 ± 0.01 mg/mL, respectively. As expected, aqueous extract exhibited the least inhibition of α-glucosidase with $IC_{50} = 1.97 \pm 0.01$ mg/mL and α-amylase with $IC_{50} = 2.01 \pm 0.01$ mg/mL. The statistical comparison revealed significant variations among different solvent extracts ($p < 0.05$). However, positive control (acarbose) had the inhibition potential which is far higher than the tested extracts. Meanwhile, maximum inhibitory potential of 80% ethanolic extract against these enzymes can be linked to higher contents of phenolic and flavonoid in this extract (Table 1).

Table 2 The IC_{50} values for α-glucosidase and α-amylase inhibition by leaf extracts of *C. procera*

Extract	α-Glucosidase inhibition IC_{50} value in mg/mL	α-Amylase inhibition IC_{50} value in mg/mL
Aqueous	1.97 ± 0.01^f	2.01 ± 0.01^g
20% ethanol	1.32 ± 0.01^e	1.76 ± 0.01^f
40% ethanol	1.12 ± 0.01^d	1.37 ± 0.02^e
60% ethanol	0.91 ± 0.01^c	1.10 ± 0.01^c
80% ethanol	0.78 ± 0.01^b	0.93 ± 0.01^b
100% ethanol	1.18 ± 0.06^d	1.31 ± 0.01^d
Acarbose	0.035 ± 0.001^a	0.038 ± 0.001^a

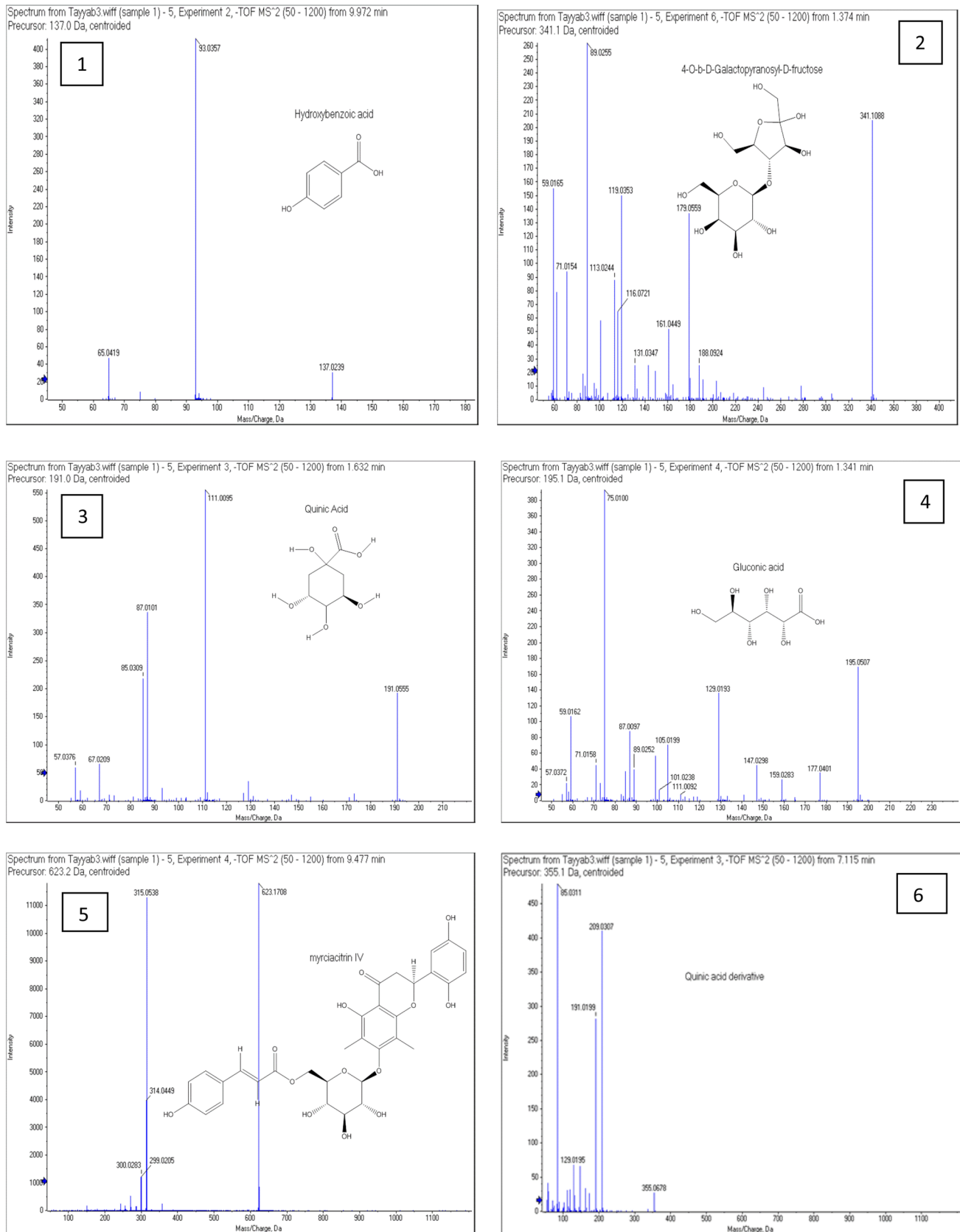**Fig. 4** Base peak chromatogram of 80% ethanol leaf extract of *C. procera* in negative ion mode

Fig. 5 UHPLC-QTOF/MS based mass spectrums of compounds identified from *C. procera*
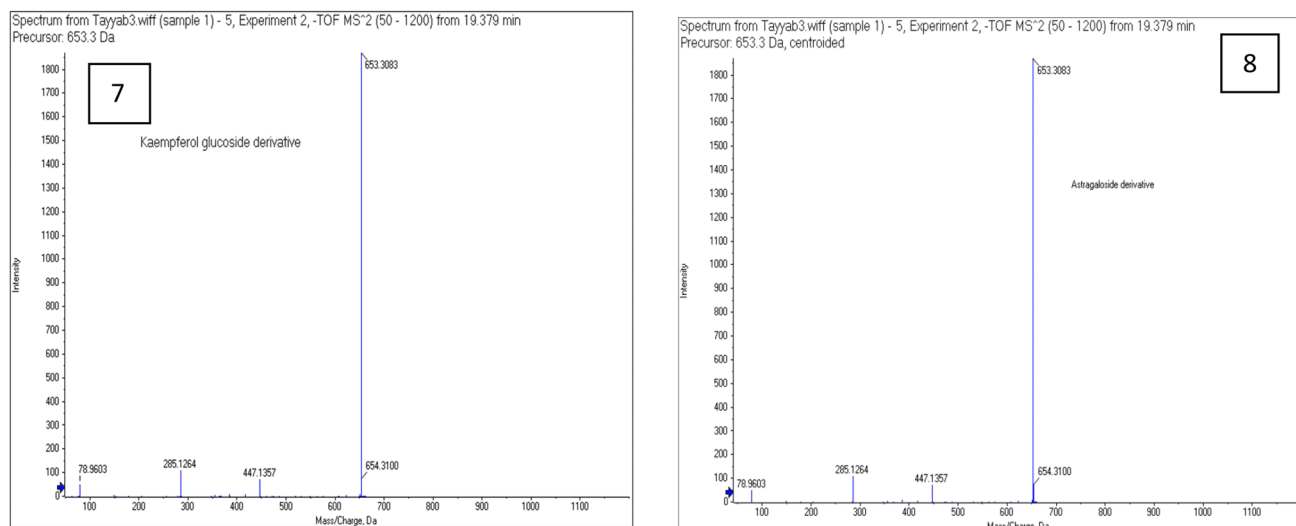
Fig. 5 (continued)

Table 3 Mass spectrometric data for identified compounds in leaf extract of *C. procera*

| S.no	t_R (minutes)	$[M–H]^-$ (m/z)	Predicted formula	Major fragments (m/z)	Identification	Classification
1	9.972	137	$C_7H_6O_3$	93, 65	Hydroxybenzoic acid	Phenolic acid
2	1.374	341	$C_{12}H_{22}O_{11}$	179, 161, 131, 119, 113	4-O-β-D-Galactopyranosyl-D-fructose	Glycoside
3	1.632	191	$C_7H_{12}O_6$	111, 85, 67, 57	Quinic acid	Organic acid
4	1.341	195	$C_6H_{12}O_7$	177, 159, 129, 101, 75, 57	Gluconic acid	Organic acid
5	9.477	623	$C_{32}H_{32}O_{13}$	314, 299	Myrciacitrin IV	Flavanone Glucoside
6	7.115	355	$C_{15}H_{16}O_{10}$	209, 191, 129, 85	Quinic acid derivative	Phenolic acid
7	19.379	653	$C_{40}H_{46}O_8$	447, 285, 79	Kaempferol glucoside derivative	Flavonol glucoside
8	19.379	653	$C_{40}H_{46}O_8$	447, 285, 79	Astragaloside derivative	Saponin

Metabolite profiling

In vitro study revealed that 80% aqueous:ethanol extract of *C. procera* leaf was most active and therefore this extract was further evaluated for profiling of potential metabolites by UHPLC-QTOF-MS/MS. The main chromatogram of UHPLC-QTOF-MS/MS is given as Fig. 4. Mass spectral analysis along with structures of identified compounds is presented as Fig. 5.

UHPLC-QTOF-MS/MS data for identified compound namely molecular ions $[M–H]^-$, major fragment ions obtained, retention times (t_R) and classes are depicted in Table 3.

The analysis of 80% ethanol extract of *C. procera* revealed the presence of eight bioactives as predominant compounds. Compound **1** generated a deprotonated $[M–H]^-$ ion (t_R = 9.972 min) at 137 in negative ionization mode [56] and a base peak $[M–H-44]^-$ at 93 via neutral loss of a CO_2 moiety from parent ion [57]. The peak at 65 might be due to cyclopentadiene anion, obtained by loss of CO molecule from ion at 93. Thus compound **1** was identified as *p*-hydroxybenzoic acid (Fig. 5; Table 3). Studies have shown *p*-hydroxybenzoic acid as an effective antioxidant (SC_{50} = 0.35 ± 0.017 mM) against various types of free radical species to counter overproduction of ROS [58, 59]. This compound has been identified in the literature to cause significant hypoglycemic effect in diabetic rats [60], increase serum insulin as well as liver glycogen levels in normal rats [60], and reported to show significant α-glucosidase inhibition potential with IC_{50} value 56.43 ± 2.09 µmol/L compared to acarbose (IC_{50} = 301.72 ± 0.21 µmol/L) [61]. α-Glucosidase inhibitors are considered as new class of antidiabetic agents. Compound **2** (Fig. 5; Table 3) appeared at 1.374 min. A molecular ion $[M–H]^-$ at 341 was shown as an intense peak. The base peak detected at 179, $[M–H-162]^-$, might be by the loss of hexose moiety ($C_6H_{10}O_5$) for example galactose/glucose/fructose. The other fragments at 161, 131, 119 and 113 supported the loss of H_2O and $–CH_2O$
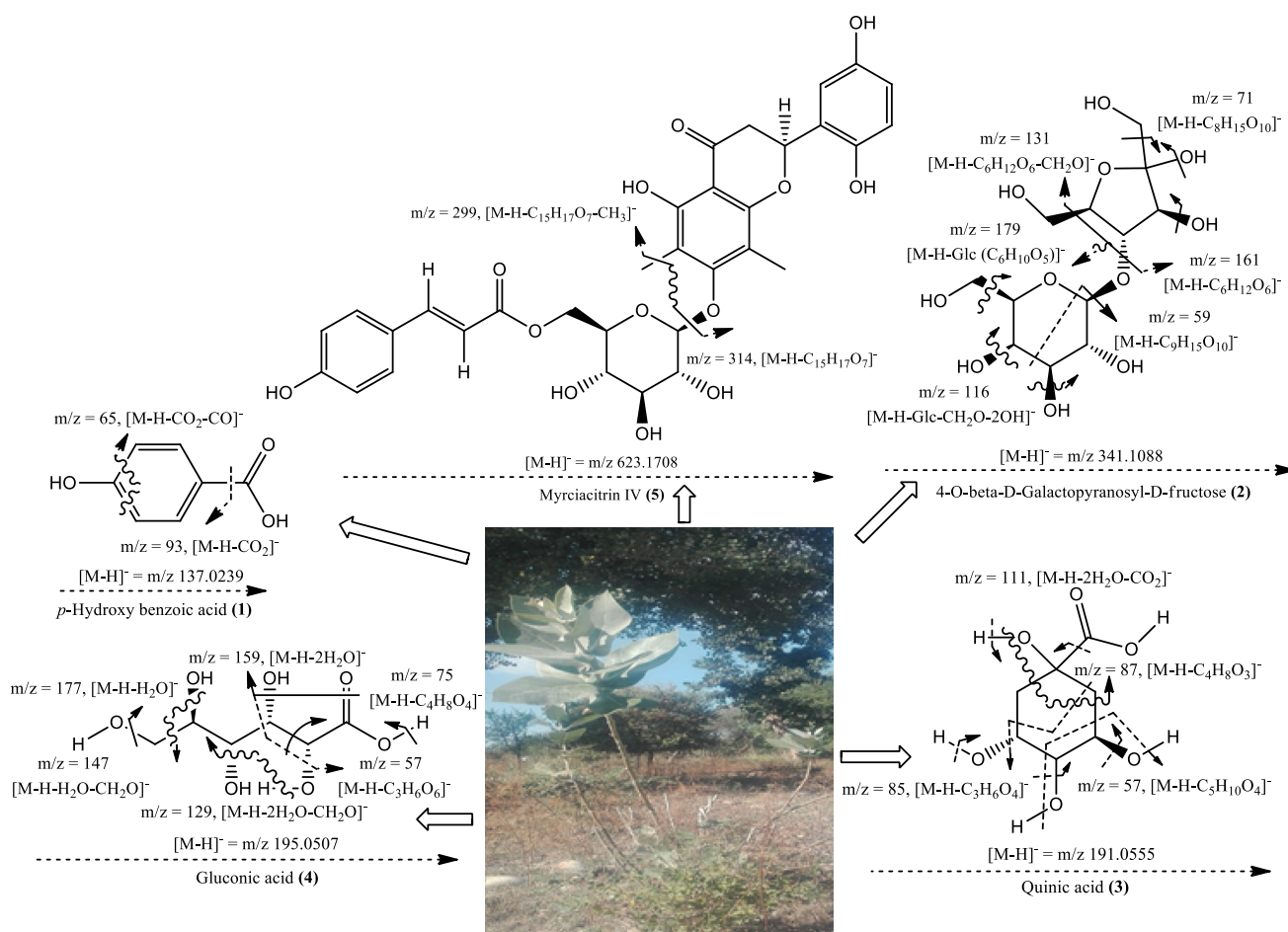
Fig. 6 Possible MS/MS fragmentation pattern of identified metabolites

groups from hexose. Based on spectral data and data already reported in literature, this compound was tentatively allocated as 4-O-β-D-galactopyranosyl-D-fructose (lactulose) [62]. In literature compound **2** was reported as an indirect antioxidant [63] and as non-digestible carbohydrate with potential prebiotic effect regarding treatment of hyperglycemia in vivo.

Prebiotics along with probiotics are proved to be very effective against various disorders/ailments once used in food applications/nutraceuticals preparations [64]. MS/MS spectrum of compound **3** at t_R 1.632 min presented diagnostic [M–H]$^-$ ion at 191. It yielded a major product ion at 111 with neutral loss of CO_2 and H_2O molecules from precursor ion [65], the other ions at 85 and 57 suggested the loss of $C_3H_6O_4$ [66] and $C_5H_{10}O_4$ moieties from molecular ion. Compound **3** was therefore identified as quinic acid and its fragmentation pathway (Fig. 6) was consistent with data from literature. A study based on rat model indicated the synergistic impact of both quinic acid and quercetin to reduce hyperglycaemia, hyperlipidemea and insulin resistance. The possible cause behind it was

the improvement in function of β-cells of pancreas, kidney and liver [67]. Some previous studies have revealed that quinic acid not only inhibit carbohydrate hydrolyzing enzymes with $IC_{50} = 1.57$ µM [64] and 4.91 µM [68] for α-amylase and $IC_{50} = 4.95$ µM for α-glucosidase [69] but also exhibit anti-oxidant potential ($IC_{50} = 663.1 \pm 7.2$ µg/mL) because of its free radical scavenging ability [70]. Compound **4** was identified as gluconic acid (pentahydroxycaproic acid) revealing diagnostic precursor [M–H]$^-$ ion at 195, with t_R 1.341 min, having further product ions at 129, [M–H–$2H_2O$–CH_2O]$^-$, 159, [M–H–$2H_2O$]$^-$, and 177, [M–H–H_2O]$^-$ corresponding to data with literature [71]. The fragment at 75 supported the loss of $C_4H_8O_4$ moiety [72] while the ion at 57 might be appeared by neutral loss of $C_3H_6O_6$ from the basic structure (Fig. 6; Table 3). It is a weak organic acid and has gained attention in food industry for formulation of hygienic food products [73]. Compound **5** was obtained at the t_R, 9.477 min. It had a precursor ion [M–H]$^-$ at 623 in UHPLC-QTOF-MS spectrum, generated a fragment ion [M–H–$C_{15}H_{17}O_7$]$^-$ at 314. It further suffered neutral loss of -CH_3 group to produce

characteristic fragment ion at 299 as reported in previous literature [74]. Compound **5** (Fig. 6; Table 3) was therefore putatively assigned as myrciacitrin IV. This compound was reported for antidiabetic activity with IC_{50} value of 7.9×10^{-7} M [75]. Finally, UHPLC-QTOF-MS analysis (Fig. 5; Table 3) suggested the presence of three derivatives namely quinic acid derivative ($t_R = 7.115$ min) presenting pseudo molecular ion $[M–H]^-$ at 355 and a product ion at 191 (quinic acid) [66] as well as kaempferol glucoside and astragaloside derivatives ($t_R = 19.379$ min), having identical precursor ions $[M–H]^-$ at 653 and product ions at 447, 285, characteristic for kaempferol glucoside/astragaloside and are in agreement with literature [76-78], but these compounds were not identified exactly, and their structures could not be proposed due to lack of enough evidence. Previous studies reveal that kaempferol glycoside, astragaloside and quinic acid derivatives possess antioxidant/antidiabetic properties [67, 79-81].

Consequently, current study suggested that 80% hydroethanolic leaf extract of *C. procera* is an important source of bioactives (phenolic acids/flavanone/glycoside/flavonol/saponin), showing the potential antioxidant, α-amylase and α-glucosidase enzyme inhibitory activity. The synthetic drugs and compounds being used to treat diabetes are associated with some serious health risks [82, 83]. The major health risks associated with metformin, sulfonylureas, thiazolidinediones and insulin include lactic acidosis, bone fracture, cardiovascular disorders, cancer and weight gain [84]. Whereas, selected plant foods are known to decrease not only blood glucose level but also control side complications of diabetes mellitus [85]. Therefore, people can shift to such natural sources with minimum or no side effects compared to synthetic drugs.

Docking studies

Docking studies on phytoconstituents of ethanolic leaf extracts of *C. procera* were carried out using our previously reported homology modelled α-glucosidase [40]. These docking simulations were made using MOE software package. The active site of model comprised of catalytic triad residues: Asp214, Glu276 and Asp349 (red sphere in Fig. 7a). The other important amino acid residues in the active site are shown in yellow spheres. Important amino acid residues in stick form are shown in Fig. 7b. First, we docked the standard acarbose in binding site of the homology-modelled α-glucosidase. The lowest energy binding pose of the acarbose is shown in Fig. 7c. The binding energy calculated for acarbose was -9.2756 kcal/mol. The important amino acid residue in contact with acarbose are: Trp59, Gln63, Arg 195, Asp197, Lys200, His201, Glu233, Glu240, Asp300, Gly306.
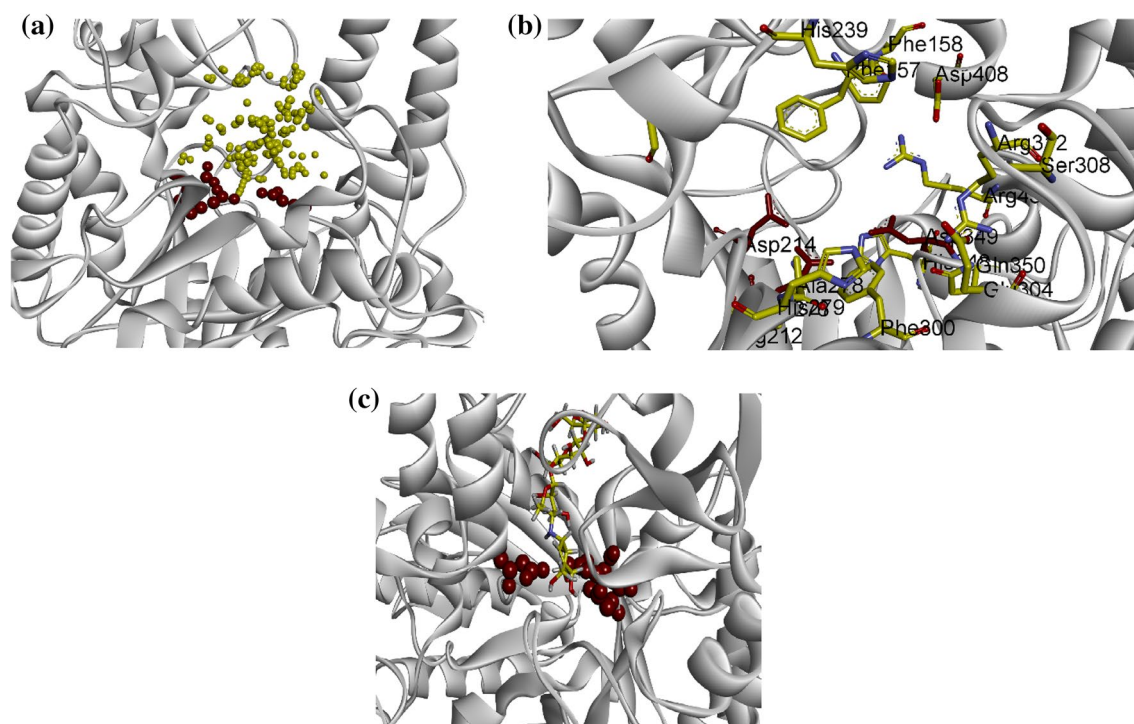
Fig. 7 **a** Ribbon diagram of homology modelled α-glucosidase. Three residues shown as red spheres are residues of catalytic triad while possible active site shown as yellow sphere; **b** Ribbon diagram showing important residues in stick representation; **c** three-dimensional docking pose of acarbose into active site of homology-modeled α-glucosidase (Color figure online)

Table 4 Binding affinity data and ligand interactions shown by possible isolated phytochemicals against porcine pancreatic α-amylase and yeast α-glucosidase

| Compound	Binding affinity (kcal/mol)	
	α-Glucosidase	α-Amylase
1	− 4.0954	− 4.2397
2	− 6.6102	− 5.9873
3	− 4.3903	− 4.4149
4	− 5.0525	− 6.0360
5	− 9.7509	− 8.5663
Acarbose	− 9.2756	− 9.5683

The molecular docking provides a great deal of possible interactions among identified compounds and active sites of enzymes, generating logical bases of possible enzyme inhibition by the complex mixture of compounds [29]. We tried to explore the synergistic effect of the identified bioactive compounds via UHPLC-QTOF-MS/MS based phytochemical characterization. Therefore, these compounds were subjected to docking simulations to evaluate their binding affinities. The binding affinity data of compounds **1** to **5** is indicated in Table 4. Three-dimensional lowest-energy binding poses and their interaction plot of identified compounds **1** and **2** are shown in Fig. 8. As shown in Fig. 8a, compound


Fig. 8 a, **c** Three-dimensional docking poses of compound **1** and **2**, respectively into active site of homology-modeled α-glucosidase. Catalytic triad residues (Asp214, Glu276 and Asp349) are indicated as red spheres; **b**, **d** detail picture of lowest energy three-dimensional docking poses of **1** and **2**, respectively (Color figure online)
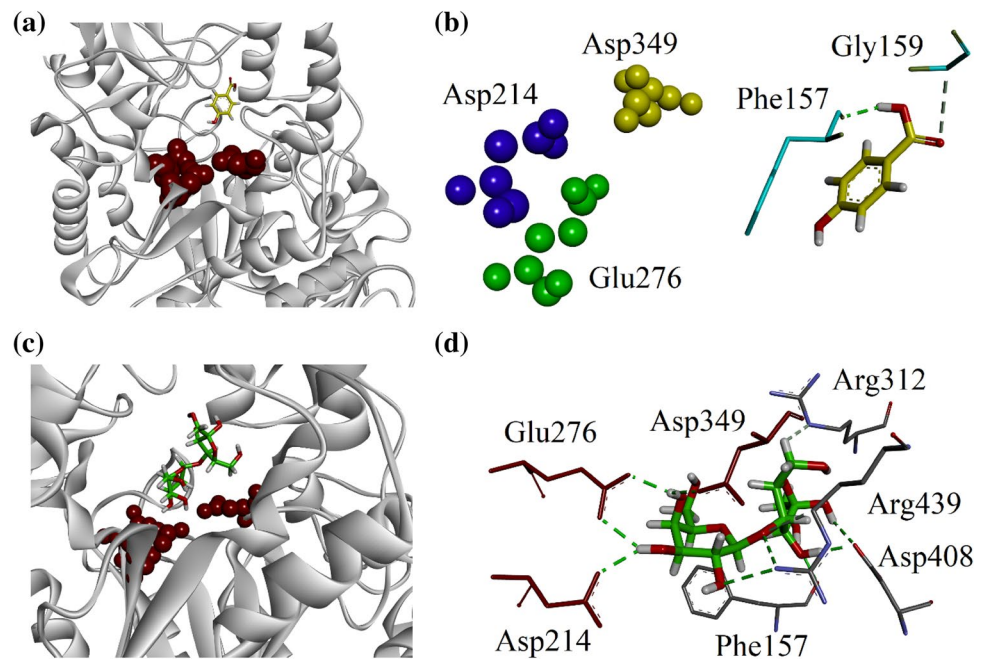
Fig. 9 a, **c** Three-dimensional docking poses of compounds **3** and **4**, respectively into an active site of homology-modeled α-glucosidase. Catalytic triad residues such as Asp214, Glu276 and Asp349 are presented in red spheres; **b**, **d** detailed picture of lowest energy three-dimensional docking poses of **1** and **2**, respectively (Color figure online)
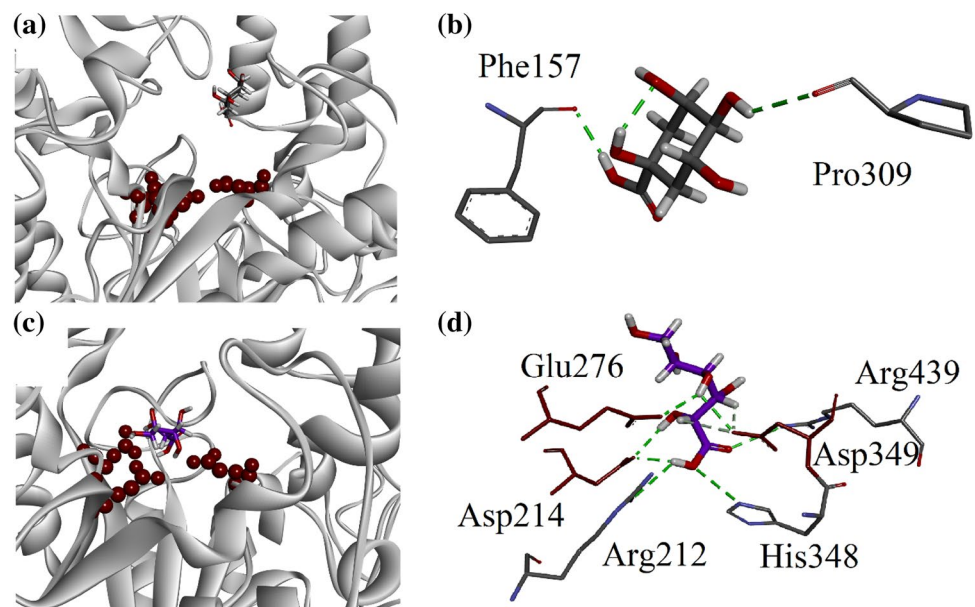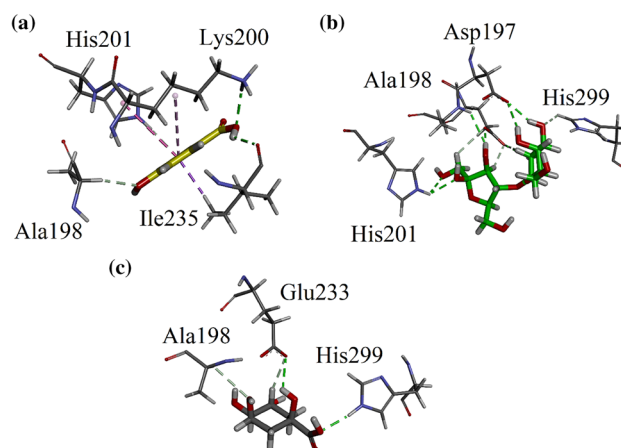
Fig. 10 **a** Three-dimensional docking poses of compound **5** into an active site of homology-modeled α-glucosidase. Catalytic triad residues as Asp214, Glu276 and Asp349 are displayed as red spheres; **b** detailed description of lowest energy three-dimensional docking pose of **5** (Color figure online)
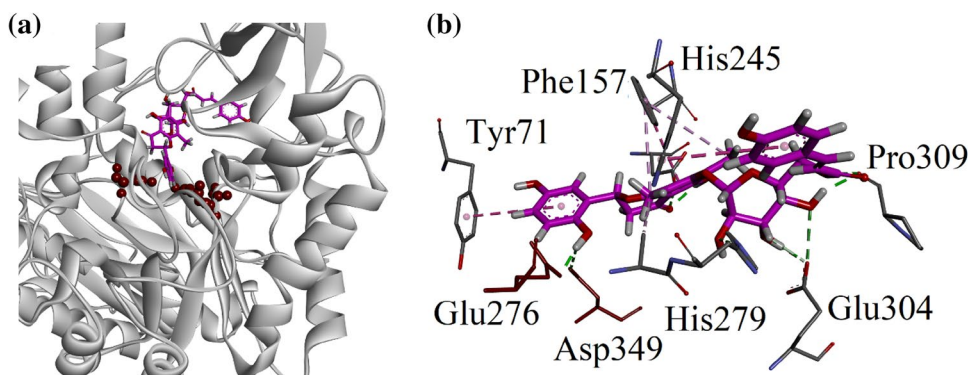
1 is docked away from catalytic triad residues (red spheres). The interaction plot shown in Fig. 8b indicates that it forms hydrogen bond (H-bond) interactions with Phe157. A weak π-alkyl bond was also observed with Gly159. The computed binding affinity for **1** is − 4.0954 kcal/mol. The lowest energy binding orientation of compound **2** showed that it binds close to the active site (Fig. 8c). Compound **2** with binding energy of − 6.6102 kcal/mol forms eight H-bond interactions via hydroxyl groups with important residues. All the three residues of catalytic triad for example Asp214, Glu276 and Asp349 establishes H-bond interactions with the hydroxyl groups. Other residues involved in H-bond are Phe157, Asp408 and Arg349 (Fig. 8d).

Binding poses of the compounds **3** and **4** are shown in Fig. 9a–d. Compound **3** binds far away from the active site and interacts with Phe157 and Pro 309 via hydrogen bond interactions (Fig. 9a, b). The computed binding affinity for **1** is − 4.3903 kcal/mol. In contrast, the orientation of the compound **4** is very close to the active site (Fig. 9c). It forms six H-bond interactions with important amino acid residues. All the catalytic triad residues established H-bonds with the compound. His348, Arg212 and Arg439 also formed H-bonds with the compound (Fig. 9d). The calculated binding affinity for compound **4** is − 5.0525 kcal/mol.

Finally, docking pose of compound **5** is shown in Fig. 10a. It binds close to the active site (Fig. 10a). Three-dimensional interaction plot showed that it forms seven H-bonds and three π–π stacking interactions. Glu276 and Asp349 forms H-bonds with one of the hydroxy groups at 2,3-dihydrochromen-4-one. Other residues involved in the H-bond interaction are Asp408, His279, Glu304 and Pro309. His245 forms π–π stacking interaction with hydroxyphenyl ring or acrylate. While Tyr71 and Phe157 forms π–π stacking interactions with 2,5-dihydroxyphenyl ring and chromone ring respectively (Fig. 10b). The computed binding affinity of the compound **5** for α-glucosidase is − 9.7509 kcal/mol. The binding affinity of compound **5** is quite comparable with recently reported binding affinity of − 9.2756 kcal/mol for acarbose against α-glucosidase [29]. However, further

Fig. 11 **a–c** Three-dimensional docking poses of compounds **1–3**, respectively into an active site of porcine pancreatic α-amylase (PDB code 1OSE)
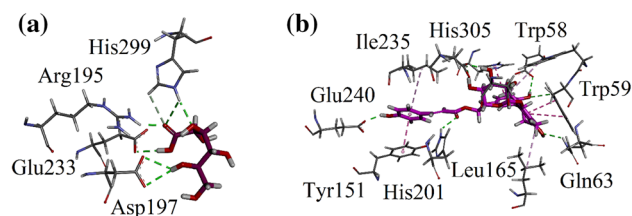
Fig. 12 **a**, **b** Three-dimensional docking poses of compounds **4** and **5**, respectively into an active site of porcine pancreatic α-amylase (PDB code 1OSE)

studies are required to examine the effect and mode of action of compound **5** towards α-glucosidase.

The identified compounds were also subjected to docking simulations against porcine pancreatic α-amylase (PDB code 1OSE) to define the role of each constituent via their computed binding affinities for important amino acid residues. The binding site of α-amylase consists of aromatic residues such as Trp58, Trp59, His101, Pro163, Ile235, Tyr258, His299, His305 and Ala307. While, the binding gorge

consist of Asp197, Glu233 and Asp300. Three-dimensional interaction plot of compounds **1–3** is shown in Fig. 11a–c. Binding affinities are tabulated in Table 4. Compound **1**, although showed weak affinity (− 4.2397 kcal/mol), showed two hydrogen bond interactions with Lys200 and Ile235 (Fig. 11a). Compound **2** with binding affinity value of − 5.9873 kcal/mol showed hydrogen bond interactions with Asp197, His201 and Glu233 (Fig. 11b). Compound **3** exhibited hydrogen bond interactions with Glu233 and His 299 (Fig. 11c).

Binding interactions of compounds **4** and **5** are shown in Fig. 12a, b. Compound **4** has shown good binding affinity value (− 6.0360 kcal/mol). The key amino acid residues involved in hydrogen bond interactions are Arg195, Asp197, Glu233 and His299 (Fig. 12a). Finally, compound **5** showed excellent binding affinity data. The computed binding affinity value of compound **5** is − 8.5663 kcal/mol. The binding orientation and interaction plot are shown in Fig. 12b. Compound **5** showed hydrogen bond as well as π–π stacking interactions. Trp59, Tyr151 and His305 showed π–π stacking interactions with phenyl rings of the compound. While, Trp59, Gln63, Asp197, His201, Glu233, Glu240 and Asp356 forms hydrogen bond interactions with hydroxy and carbonyl oxygen of the compound, furthermore suggested that compound **5** has a binding affinity (− 8.5663 kcal/mol) towards α-amylase comparable to that of acarbose (− 9.5683 kcal/mol), thus supporting that compound 5 is excellent binder of α-amylase, as shown in this work. Yet, further investigations are needed to evaluate the effect as well as the mode of action of compound **5** on α-amylase.

Present study provides a deep exploration of molecular modulation between two target enzymes and functional metabolites identified in *C. procera*. It is evident from above binding affinity data that compounds **1–5** can inhibit α-glucosidase and α-amylase synergistically to prevent hyperglycemia.

Conclusion

In the present work, UHPLC-QTOF/MS confirmed the identification of antioxidant/antidiabetic bioactive compounds in 80% ethanolic extract of *C. procera*. Based on this analysis, a total of 8 compounds including three derivatives were characterized for the first time. The antioxidant activities and enzyme inhibitory properties of understudy plant extract, supported by the presence of related bioactives, confirmed the traditional uses of this species to treat hyperglycemia. The secondary metabolites present in leaves of *C. procera* were probably responsible for antioxidant and antidiabetic effect. This study supports the potential uses of *C. procera* for development of functional foods and antioxidant/antidiabetic nutraceuticals. The experimental in vitro results were further correlated by docking simulation to explore the mechanism as well as role of each

phytochemicals in the extract. Based on the binding affinity data, we are in opinion that the constituents of *C. procera* can prevent hyperglycemia due to their synergist effect.

References

1. J. Naveen, V. Baskaran, Eur. J. Nutr. **57**, 1275–1299 (2018)
2. T. Gull, F. Anwar, B. Sultana, W. Nouman, Ind. Crops Prod. **67**, 81–96 (2015)
3. G. Muhammad, M.A. Hussain, F. Anwar, M. Ashraf, A.H. Gilani, Phytother. Res. **29**, 1–13 (2015)
4. J. Tuomilehto, P. Schwarz, J. Lindström, Diabetes Care **34**, S210–S214 (2011)
5. J. Montonen, R. Jarvinen, M. Heliovaara, A. Reunanen, A. Aromaa, P. Knekt, Eur. J. Clin. Nutr. **59**, 441 (2005)
6. J.S. de Munter, F.B. Hu, D. Spiegelman, M. Franz, R.M. van Dam, PLOS Med. **4**, 261 (2007)
7. S.K. Chang, C. Alasalvar, F. Shahidi, J. Funct. Foods **21**, 113–132 (2016)
8. F. Giacco, M. Brownlee, Circ. Res. **107**, 1058–1070 (2010)
9. L. Guariguata, D.R. Whiting, I. Hambleton, J. Beagley, U. Linnenkamp, J.E. Shaw, Diabetes Res. Clin. Pract. **103**, 137–149 (2014)
10. A. Hussain, I. Ali, Arch. Pharma. Pract. **7**, 30 (2016)
11. P. Reka, T. Banu, M. Seethalakshmi, Int. J. Pharm. Pharm. Sci. **9**, 64–68 (2017)
12. L. Zhang, Z.C. Tu, X. Xie, Y. Lu, Z.X. Wang, H. Wang, X.M. Sha, Ind. Crops Prod. **89**, 522–532 (2016)
13. F.L. Diaz-Gutierrez, J.M. Ladero, M. Diaz-Rubio, Am. J. Gastroenterol. **93**, 481 (1998)
14. M.A. Ibrahim, N.A. Koorbanally, M.S. Islam, Acta Pharm. **64**, 311–324 (2014)
15. S.A. Raza, A.R. Chaudhary, M.W. Mumtaz, A. Ghaffar, A. Adnan, A. Waheed, Pak. J. Pharm. Sci. **80**, 472–479 (2018)
16. M. Kenganora, M. Bhaskaran, M.N. Santhepete, V.I. Hukkeri, Free Radic. Antioxid. **7**, 143–151 (2017)
17. K.M. Ahmed, A. Rana, V. Dixit, Pharmacogn. Magn. **1**, 48 (2005)
18. M.N. Yesmin, S.N. Uddin, S. Mubassara, M.A. Akond, Am. Eurasian J. Agric. Environ. Sci. **4**, 550–553 (2008)
19. Z. Iqbal, M. Lateef, A. Jabbar, G. Muhammad, M.N. Khan, J. Ethnopharmacol. **102**, 256–261 (2005)
20. S. Roy, R. Sehgal, B. Padhy, V. Kumar, J. Ethnopharmacol. **102**, 470–473 (2005)
21. S.S. Ramachandra, A.A. Quereshi, A.S. Viswanath, T. Patil, T. Prakash, K. Prabhu, A.G. Veeran, Fitoterapia **78**, 451–454 (2007)
22. J.V. Kamath, A. Rana, Fitoterapia **73**, 111–115 (2002)
23. A. Basu, T. Sen, R. Ray, A.N. Chaudhuri, Fitoterapia **63**, 507–514 (1992)
24. M. Kamal, M. Adnan, W. Murad, H. Bibi, A. Tariq, H. Rahman, Z.K. Shinwari, Pak. J. Bot. **48**, 399–413 (2016)
25. B. Yogi, S.K. Gupta, A. Mishra, Bull. Environ. Pharmacol. Life Sci. **5**, 74–81 (2016)
26. P. Sharma, J. Sharma, Fitoterapia **71**, 77–79 (2000)
27. Y. Murti, S. Sharma, P. Mishra, Asian J. Pharm. Clin. Res. **8**, 188–190 (2015)
28. Y. Murti, B. Yogi, D. Pathak, J. Pharm. Res. **4**, 3452–3454 (2011)
29. M. Arshad, M.W. Mumtaz, A.R. Chaudhary, U. Rashid, M. Ali, H. Mukhtar, A. Adnan, S.A. Raza, Pak. J. Pharm. Sci. **32**, 871–874 (2019)

30. R. Pandey, B. Kumar, J. Liq. Chromatogr. Relat. Technol. **39**, 225–238 (2016)
31. J.F. Tang, W.X. Li, X.J. Tan, P. Li, X.H. Xiao, J.B. Wang, M.J. Zhu, X.I. Li, F. Meng, Anal. Methods **8**, 2904–2914 (2016)
32. M.H. Al-Zuaidy, A.A. Hamid, A. Ismail, S. Mohamed, A.F. Abdul Razis, M.W. Mumtaz, S.Z. Salleh, J. Food Sci. 81, C1080–C1090 (2016).
33. D.O. Kim, S.W. Jeong, C.Y. Lee, Food Chem. **81**, 321–326 (2003)
34. Y.S. Park, S.T. Jung, S.G. Kang, B.G. Heo, P. Arancibia-Avila, F. Toledo, J. Drzewiecki, J. Namiesnik, S. Gorinstein, Food Chem. **107**, 640–648 (2008)
35. P. Kumar, P. Kalita, T. Barman, T. Chatterjee, J. Pharm. Res. **1**, 27–35 (2013)
36. L.L. Mensor, F.S. Menezes, G.G. Leitao, A.S. Reis, T.C.d. Santos, C.S. Coube, S.G. Leitao, Phytother. Res. **15**, 127–130 (2001)
37. M. Umamaheswari, T. Chatterjee, Afr. J. Tradit. Complement. Altern. Med. **5**, 61–73 (2008)
38. L.J. Shai, P. Masoko, M.P. Mokgotho, S.R. Magano, A. Mogale, N. Boaduo, J.N. Elof, S. Afr. J. Bot. **76**, 465–470 (2010)
39. B. Jabeen, N. Riaz, M. Saleem, M.A. Naveed, M. Ashraf, U. Alam, H.M. Rafiq, R.B. Tareen, A. Jabbar, Phytochemistry **96**, 443–448 (2013)
40. M. Ali, S. Ali, M. Khan, U. Rashid, M. Ahmad, A. Khan, A. Al-Harrasi, F. Ullah, A. Latif, Bioorg. Chem. **80**, 472–479 (2018)
41. F. Iftikhar, F. Yoqoob, N. Tabassum, M.S. Jan, A. Sadiq, S. Tahir, T. Batool, B. Niaz, F.L. Ansari, M.I. Chaudhary, Bioorg. Chem. **80**, 99–111 (2018)
42. Dassault Systèmes. Discovery Studio Modeling Environment, Release 2017 (Dassault Systèmes, San Diego, 2017)
43. Y. Liu, X.R. She, J.B. Huang, M.C. Liu, M.E. Zhan, Food Sci. Technol. **38**, 1–8 (2017)
44. P.D. Duh, Y.Y. Tu, G.C. Yen, LWT-. Food Sci. Technol. **32**, 269–277 (1999)
45. M.I. Kazeem, A.M. Mayaki, B.F. Ogungbe, A.B. Ojekale, Iran. J. Pharm. Res. **15**, 37 (2016)
46. A. Gonzalez-Sarrías, L. Li, N.P. Seeram, J. Funct. Foods **4**, 185–196 (2012)
47. F. Odabasoglu, A. Aslan, A. Cakir, H. Suleyman, Y. Karagoz, M. Halici, Y. Bayir, Phytother. Res. **18**, 938–941 (2004)
48. P. Putnik, J. Lorenzo, F. Barba, S. Roohinejad, A. Rezek Jambrak, D. Granato, D. Montesano, D. Bursac Kovacevic, Foods **7**, 106 (2018)
49. Q.W. Zhang, L.G. Lin, W.C. Ye, Chin. Med. **13**, 20 (2018)
50. G. Nireesha, L. Divya, C. Sowmya, N. Venkateshan, M.N. Babu, V. Lavakumar, Int. J. Novel Trends Pharm. Sci. **3**, 87–98 (2013)
51. U. Rashid, M.R. Khan, Biomed. Pharmacother. **88**, 469–479 (2017)
52. O.B. Afolabi, O.I. Oloyede, A.A. Ojo, A.A. Onansanya, S.O. Agunbiade, B.O. Ajiboye, J. Johnson, O.A. Peters, Potr. Slovak J. Food Sci. **12**, 413–421 (2018)
53. A.B. Aliyu, M.A. Ibrahim, A.M. Musa, A.O. Musa, J.J. Kiplimo, A.O. Oyewale, Acta Pol. Pharm. **70**, 115–121 (2013)
54. V. Ghadyale, S. Takalikar, V. Haldavnekar, A. Arvindekar, Evid. Based Complement. Altern. Med. **2012**, 1–6 (2012)
55. S.K. Singh, P.K. Rai, D. Jaiswal, G. Watal, Evid. Based Complement. Altern. Med. **5**, 415–420 (2008)
56. Y. Du, Z. Wang, L. Wang, M. Gao, L. Wang, C. Gan, C. Yang, Molecules **22**, 1494 (2017)
57. J. Sun, F. Liang, Y. Bin, P. Li, C. Duan, Molecules **12**, 679–693 (2007)

58. A. Yarizade, A. Niazi, H.H. Kumleh, J. Pharm. Sci. Res. **9**, 2382–2387 (2017)
59. V. Chandrasekar, P.D. Belur, I. Regupathi, Resour. Efficient Technol. **2**, S114–S118 (2016)
60. P. Peungvicha, R. Temsiririrkkul, J.K. Prasain, Y. Tezuka, S. Kadota, S.S. Thirawarapan, H. Watanabe, J. Ethnopharmacol. **62**, 79–84 (1998)
61. Z. Yin, W. Zhang, F. Feng, Y. Zhang, W. Kang, Food Sci. Hum. Wellness **3**, 136–174 (2014)
62. H.G. Agalar, G.A. Ciftci, F. Goger, N. Kırımer, Rec. Nat. Prod. **12**, 64–75 (2017)
63. X. Chen, Q. Zuo, Y. Hai, X.J. Sun, Med. Hypotheses **76**, 325–327 (2011)
64. A. Bhatia, G. Kaur, M. Kaur, R. Singla, Adv. Appl. Sci. Res. **3**, 3020–3024 (2012)
65. J.B. Chang, M.E. Lane, M. Yang, M. Heinrich, Planta Med. **82**, 1134–1141 (2016)
66. N.P. Kalogiouri, N.A. Alygizakis, R. Aalizadeh, N.S. Thomaidis, Anal. Bioanal. Chem. **408**, 7955–7970 (2016)
67. A. Arya, M.M.J. Al-Obaidi, N. Shahid, M.I.B. Noordin, C.Y. Looi, W.F. Wong, S.L. Khaing, M.R. Mustafa, Food Chem. Toxicol. **71**, 183–196 (2014)
68. S. Santhosh, Int. J. Pharm. Sci. Res. **6**, 2127–2132 (2015)
69. S. Das, J. Acharya, B. De, Int. J. Food Prop. **20**, 2982–2993 (2017)
70. D.P. Singh, S. Verma, R. Prabha, J. Plant Biochem. Physiol. **6**, 1–5 (2018)
71. M. de la Luz Cadiz-Gurrea, S. Fernández-Arroyo, J. Joven, A. Segura-Carretero, Food Res. Int. 50, 197–204 (2013).
72. A. Duangjai, N. Suphrom, J. Wungrath, A. Ontawong, N. Nuengchamnong, A. Yosboonruang, Integr. Med. Res. **5**, 324–331 (2016)
73. S. Ramachandran, P. Fontanille, A. Pandey, C. Larroche, Food Technol. Biotechnol. **44**, 185–195 (2006)
74. H. Matsuda, N. Nishida, M. Yoshikawa, Chem. Pharm. Bull. **50**, 429–431 (2002)
75. G. Brahmachari, Res. Signpost **661**, 187–212 (2011)
76. S. Kumar, A. Singh, B. Kumar, J. Pharm. Anal. **7**, 214–222 (2017)
77. M.E. Karar, N. Kuhnert, J. Chem. Biol. Ther. **1**, 102 (2015)
78. G. Chen, X. Li, F. Saleri, M. Guo, Molecules **21**, 1275 (2016)
79. R. Yang, Y. Guan, W. Wang, H. Chen, Z. He, A.Q. Jia, PLoS ONE **13**, 1–20 (2018)
80. M. Zhang, W.X. Liu, M.F. Zheng, Q.L. Xu, F.H. Wan, J. Wang, T. Lei, Z.Y. Zhou, J.W. Tan, Molecules **18**, 14096–14104 (2013)
81. L. Lv, S.Y. Wu, G.F. Wang, J.J. Zhang, J.X. Pang, Z.Q. Liu, W. Xu, S.G. Wu, J.J. Rao, Phytother. Res. **24**, 219–224 (2010)
82. W. Kooti, M. Farokhipour, Z. Asadzadeh, D. Ashtary-Larky, M. Asadi-Samani, Electron. Phys. **8**, 1832 (2016)
83. R.C. Gupta, D. Chang, S. Nammi, A. Bensoussan, K. Bilinski, B.D. Roufogalis, Diabetol. Metab. Syndr. **9**, 59 (2017)
84. C.R. Triggle, H. Ding, Ther. Adv. Chronic Dis. **5**, 245–268 (2014)
85. G. Subbulakshmi, M. Naik, Bombay Hosp. J. **43**, 548–561 (2001)